Electrochimica Acta xxx (2010) xxx–xxx

Contents lists available at ScienceDirect

Electrochimica Acta

journal homepage: www.elsevier.com/locate/electacta

Insights on the SO_2 poisoning of Pt_3Co/VC and Pt/VC fuel cell catalysts

Olga A. Baturina [a,*], Benjamin D. Gould [a], Yannick Garsany [a,b], Karen E. Swider-Lyons [a]

[a] Naval Research Laboratory, Code 6113, Washington, DC 20375, United States
[b] EXCET, Inc., Springfield, VA 22151, United States

ARTICLE INFO

Article history:
Received 13 January 2010
Received in revised form 7 May 2010
Accepted 4 June 2010
Available online xxx

Keywords:
SO_2 poisoning
Carbon-supported Pt_3Co catalyst
Rotating disk electrode
Platinum electrochemical surface area
Proton exchange membrane fuel cell

ABSTRACT

SO_2 poisoning of carbon-supported Pt_3Co (Pt_3Co/VC) catalyst is performed at the cathode of proton exchange membrane fuel cells (PEMFCs) in order to link previously reported results at the electrode/solution interface to the FC environment.

First, the surface area of Pt_3Co/VC catalyst is rigorously characterized by hydrogen adsorption, CO stripping voltammetry and underpotential deposition (*upd*) of copper adatoms. Then the performance of PEMFC cathodes employing 30 wt.% Pt_3Co/VC and 50 wt.% Pt/VC catalysts is compared after exposure to 1 ppm SO_2 in air for 3 h at constant cell voltage of 0.6 V. In agreement with results reported for the electrode/solution interface, the Pt_3Co/VC is more susceptive to SO_2 poisoning than Pt/VC at a given platinum loading.

Both catalysts can be recovered from adsorbed sulfur species by running successive polarization curves in air or cyclic voltammetry (CV) in inert atmosphere. However, the activity of Pt_3Co/VC having ~3 times higher sulfur coverage is recovered more easily than Pt/VC. To understand the difference between the two catalysts in terms of activity recovery, platinum–sulfur interaction is probed by thermal programmed desorption at the catalyst/inert gas interface and CV at the electrode/solution interface and in the FC environment.

Published by Elsevier Ltd.

1. Introduction

In our previous paper [1], the effect of SO_2 on the oxygen reduction reaction (ORR) was compared for 30 wt.% Pt_3Co/VC (BASF, developmental) and 20 wt.% Pt/VC (E-TEK) catalysts using CV and rotating ring-disk electrode (RRDE) techniques. We found that a 30 wt.% Pt_3Co/VC catalyst is more susceptive to SO_2 poisoning at a given platinum loading. It was evidenced by a higher coverage of the platinum surface by adsorbed sulfur species after exposure of the Pt_3Co/VC thin-film electrodes to S(IV) aqueous solution. However, compared to Pt/VC [1,2], it was easier to recover Pt_3Co/VC from adsorbed sulfur species both by running successive polarization curves in oxygen and CV in inert atmosphere, meaning that fewer cycles were needed to get initial mass-activity for ORR or to clean the surface from adsorbed sulfur species in inert atmosphere. We assumed that adsorbed sulfur species are more easily removed from Pt_3Co/VC surface due to a weaker platinum–sulfur bonding indicated by density functional theory (DFT) [3,4]. The assumption about weaker platinum–sulfur bond for Pt_3Co alloy seems obvious, knowing that platinum–oxygen bond is weaker for this catalyst [5] and that both sulfur and oxygen belong in the same group of the periodic table of elements. This assumption has never been experimentally proven, though.

Here we extend our previous findings to SO_2 poisoning of 30 wt.% Pt_3Co/VC and 50 wt.% Pt/VC electrocatalysts (used by Ion Power, Inc. for making commercial catalyst coated membranes (CCMs)) at the fuel cell cathodes. We start with characterization of electrocatalytic activities of 30 wt.% Pt_3Co/VC, 20 wt.% Pt/VC and 50 wt.% Pt/VC towards ORR at electrode/solution interface in order to compare them with the activities of 30 wt.% Pt_3Co/VC and 50 wt.% Pt/VC in $H_2|O_2$ fuel cells. The 20 wt.% Pt/VC catalyst is investigated in order to gain a better understanding of the Pt particle size effect, as platinum particle size for this catalyst (3.5 ± 0.3 nm) is between particle sizes of the 30 wt.% Pt_3Co/VC and the 50 wt.% Pt/VC (4.3 ± 0.3 and 2.9 ± 0.5 nm, respectively). To eliminate uncertainties in platinum electrochemical surface area (ECSA) determination caused by double layer correction and possible hydrogen spillover [6], the surface areas of the above three catalysts in an electrochemical cell are determined by three different methods: hydrogen adsorption (H-adsorption), CO stripping voltammetry and Cu-*upd*. In fuel cell experiments, only the H-desorption method is implemented.

In order to compare the SO_2 poisoning of 30 wt.% Pt_3Co/VC and 50 wt.% Pt/VC in fuel cells, SO_2 poisoning of cathode catalysts is performed with 1 ppm SO_2 in air for 3 h while holding the cell volt-

* Corresponding author at: Naval Research Laboratory, Chemistry Division, Code 6113, 4555 Overlook Ave SW, Washington, DC 20375, United States. Tel.: +1 202 767 2631.
E-mail address: olga.baturina@nrl.navy.mil (O.A. Baturina).

0013-4686/$ – see front matter. Published by Elsevier Ltd.
doi:10.1016/j.electacta.2010.06.004

Report Documentation Page

Form Approved
OMB No. 0704-0188

1. REPORT DATE	2. REPORT TYPE	3. DATES COVERED
07 MAY 2010		**00-00-2010 to 00-00-2010**

4. TITLE AND SUBTITLE	5a. CONTRACT NUMBER
Insights on the SO2 poisoning of Pt3Co/VC and Pt/VC fuel cell catalysts	5b. GRANT NUMBER
	5c. PROGRAM ELEMENT NUMBER
6. AUTHOR(S)	5d. PROJECT NUMBER
	5e. TASK NUMBER
	5f. WORK UNIT NUMBER
7. PERFORMING ORGANIZATION NAME(S) AND ADDRESS(ES) **Naval Research Laboratory,Code 6113,Washington,DC,20375**	8. PERFORMING ORGANIZATION REPORT NUMBER
9. SPONSORING/MONITORING AGENCY NAME(S) AND ADDRESS(ES)	10. SPONSOR/MONITOR'S ACRONYM(S)
	11. SPONSOR/MONITOR'S REPORT NUMBER(S)

12. DISTRIBUTION/AVAILABILITY STATEMENT
Approved for public release; distribution unlimited

13. SUPPLEMENTARY NOTES

14. ABSTRACT

SO2 poisoning of carbon-supported Pt3Co (Pt3Co/VC) catalyst is performed at the cathode of proton exchange membrane fuel cells(PEMFCs)in order to link previously reported results at the elec-trode/solution interface to the FC environment. First, the surface area of Pt3Co/VC catalyst is rigorously characterized by hydrogen adsorption,CO stripping voltammetry and under potential deposition(upd) of copper adatoms.Then the performance of PEMFC cathodes employing 30wt.%Pt3Co/VC and 50wt.%Pt/VC catalysts is compared after exposure to 1ppmSO2 in air for 3 h at constant cell voltage of 0.6V.In agreement with results reported for the electrode/solution interface,thePt3Co/VC is more susceptive to SO2 poisoning than Pt/VC at a given platinum loading. Both catalysts can be recovered from adsorbed sulfur species by running successive polarization curves in air or cyclic voltammetry (CV)in inert atmosphere.However,the activity of Pt3Co/VC having ∼3 times higher sulfur coverage is recovered more easily than Pt/VC.To understand the difference between the two catalysts in terms of activity recovery,platinum?sulfur interaction is probed by thermal programmed desorption at the catalyst/inert gas interface and CV at the electrode/solution interface and in the FC environment.

15. SUBJECT TERMS

16. SECURITY CLASSIFICATION OF:			17. LIMITATION OF ABSTRACT	18. NUMBER OF PAGES	19a. NAME OF RESPONSIBLE PERSON
a. REPORT **unclassified**	b. ABSTRACT **unclassified**	c. THIS PAGE **unclassified**	**Same as Report (SAR)**	**11**	

age at 0.6 V. The same protocol was used in our previous paper [7] where the voltage effect on SO_2 adsorption at the PEMFC cathodes was investigated. The extent of SO_2 poisoning is evaluated based on performance degradation and coverage of the platinum surface by adsorbed sulfur species after exposure of both cathode catalysts to SO_2. Coverage of sulfur species is determined from suppression of the hydrogen desorption region on the CVs. As the platinum ECSAs of the 30 wt.% Pt_3Co/VC and 50 wt.% Pt/VC catalysts are a factor of two different, the SO_2 poisoning effect is studied both at constant platinum loading (fuel cell) and identical platinum surface areas (electrochemical cell). Finally, recovery strategies are discussed and the platinum–sulfur bonding is probed by temperature programmed desorption (TPD) at the catalyst/gas phase interface in order to verify that the platinum–sulfur bond is weaker for the Pt_3Co/VC catalyst.

2. Experimental

2.1. Rotating disk electrode (RDE) experiments

The electrocatalytic activities of the 20 wt.% Pt/VC (E-TEK, currently BASF), 50 wt.% Pt/VC (purchased from Ion Power, Inc.; information about manufacturer is not disclosed) and 30 wt.% Pt_3Co/VC (BASF, developmental) catalysts towards the ORR were evaluated in a standard three-electrode electrochemical cell using the thin-film RDE technique [8]. A thin film of the catalyst was deposited on the tip of a glassy carbon electrode (5 mm diameter, Pine Instruments) that served as a working electrode (WE). The rotation of the WE was implemented by a rotator (Pine Instruments, AFCPRB). A platinum mesh and a home-made reversible hydrogen electrode (RHE) were used as counter and reference electrodes, respectively. The RHE was separated from the main compartment of the cell by a bridge with electrolyte connected to the cell via a Luggin capillary. A solution of 0.1 M $HClO_4$ prepared from double distilled perchloric acid (GFS Chemicals) was used as the working electrolyte. The electrolyte was purged with ultra high purity (UHP) oxygen (4.3 grade, GTS-Welco) for 20 min prior to measuring the ORR curves. During ORR measurements, the flow of oxygen through electrolyte was replaced by a flow above the electrolyte, to create an oxygen "blanket". The ORR measurements were performed at a rotation rate of 1600 rpm and scan rates of 5 and 20 mV s^{-1} at room temperature.

The platinum loading was 20 μg_{Pt} cm^{-2} for the 30 wt.% Pt_3Co/VC and the 20 wt.% Pt/VC and 30 μg_{Pt} cm^{-2} for 50 wt.% Pt/VC. The higher platinum loading for the 50 wt.% Pt/VC was used because we were unable to obtain good uniform films with a Pt loading of 20 μg_{Pt} cm^{-2}. Catalyst inks were prepared by dispersing 15–20 mg of the catalysts in 10 mL of an ink solution [8]. Homogeneous catalyst distribution in the ink was achieved by 1 h sonication in an ultrasonic bath sonicator (Branson 2510). A 8–10 μL aliquot of the ink was pipetted on the tip of the glassy carbon electrode to get the desired platinum loading. Thin uniform films were obtained after drying the glassy carbon electrodes in air at room temperature.

All potentials measured in the electrochemical cell are reported with respect to RHE in 0.1 M $HClO_4$ at atmospheric H_2 pressure.

To evaluate the electrocatalytic activities of both catalysts towards the ORR, kinetic currents were extracted from the total currents according to Eq. (1) [9]:

$$I_k = \frac{I_d \cdot I}{I_d - I} \quad (1)$$

where I is the total current and I_d is the limiting diffusion current. Mass- and area-specific activities were determined by normalization of I_k to the electrode's platinum loading (μg_{Pt}) and platinum ECSA ($cm^2{}_{Pt}$), respectively.

2.2. Platinum ECSA determination

Platinum ECSAs of the thin-film electrodes were determined by three different methods: hydrogen adsorption, CO stripping voltammetry and Cu-*upd*.

2.2.1. Pt ECSA evaluation from the hydrogen adsorption region

Electrodes were electrochemically cleaned in N_2-purged electrolyte solution by cycling the potential of the WE between 0 and 1.4 V at a scan rate of 500 mV s^{-1} until reproducible voltammograms were obtained (typically 20 cycles). Then, CVs were recorded in the potential range of 0.05–1.1 V (vs. RHE) at scan rates of 20, 50 and 100 mV s^{-1}. The platinum ECSAs were calculated from the hydrogen adsorption region on CVs after correction for double layer charging (subtraction of the current measured at 0.4 V vs. RHE from the total current). To avoid the influence of H_2 evolution on the hydrogen adsorption region, integration was performed between 0.065 and 0.4 V for the 30 wt.% Pt_3Co/VC, 0.06 and 0.4 V for the 20 wt.% Pt/VC, and 0.05 and 0.4 V for 50 wt.% Pt/VC. 210 [9] and 200 $\mu C\ cm^{-2}{}_{Pt}$ [10] were used as a conversion factor for Pt/VC and Pt_3Co/VC thin films, respectively. ECSAs determined from CVs recorded at 20, 50 and 100 mV s^{-1} were consistent within ±5%.

2.2.2. CO stripping voltammetry

To implement the second method [11–13], the potential of electrochemically cleaned electrodes in O_2-free electrolyte was set to 0.06 V vs. RHE. Then UHP CO (GTS-Welco) was introduced for 30 min while holding the WE under potential control. Following that, the solution was purged with research grade N_2 (6.0, GTS-Welco) for 30 min to remove dissolved CO. Then two voltammetric scans were carried out according to the following program: 0.06 V → 1.3 V → 0.05 V → 0.06 V at a scan rate of 10 mV s^{-1}. To evaluate the platinum ECSA, the area under the CO stripping peak was calculated after subtraction of background current observed during the 2nd positive sweep from the current measured during the 1st positive sweep. Integration limits were 0.55 and 1.1 V. As two electrons per CO molecule are consumed to oxidize CO to CO_2 [14], 420 and 400 $\mu C\ cm^{-2}{}_{Pt}$ were used to convert the charge consumed for a monolayer of CO oxidation into platinum ECSA for Pt/VC and Pt_3Co/VC films, respectively.

2.2.3. Cu-upd

The similar size of platinum and copper atoms (Pt and Cu atomic radii are 0.139 and 0.128 nm, respectively [15]) makes copper underpotential deposition a perfect tool for evaluating the platinum ECSA. An experimental technique was adopted from the literature [6,15,16]. First, the thin-film electrode was held at 0.06 V for 15 min in a degassed 0.1 M $HClO_4$ electrolyte. Then its potential was moved stepwise to 0.33 V, and a background potentiodynamic scan was recorded between 0.33 and 1.3 V at 1 mV s^{-1}. The procedure was repeated one more time, but this time a stock solution of $CuSO_4{\cdot}5H_2O$ (99.999% assay, GFS Chemicals) was introduced into the cell (to produce 0.005 M $CuSO_4$ in the cell) while the WE was under potential control at 0.33 V. To facilitate diffusion of cupric ions to the electrode surface, the rotator was turned on at 1600 rpm when the cupric solution was introduced into the cell. In order to obtain a monolayer of Cu adatoms on the surface of the platinum nanoparticles, the electrode was kept under potential control for 30 min while the solution was degassed with research grade N_2. Finally, Cu stripping was performed by sweeping the potential from 0.33 to 1.3 V at 1 mV s^{-1}. The charge consumed for the oxidation of copper adatoms was determined by integration of the current vs. time curve, obtained by subtraction of the background current (measured in a clean 0.1 M $HClO_4$) from current measured in the presence of cupric ions in solution. The platinum ECSA was calculated assuming that a monolayer coverage of platinum by cop-

Please cite this article in press as: O.A. Baturina, et al., Insights on the SO_2 poisoning of Pt_3Co/VC and Pt/VC fuel cell catalysts, Electrochim. Acta (2010), doi:10.1016/j.electacta.2010.06.004

per adatoms is achieved and copper oxidation requires $2e^-$, i.e. using 420 and 400 $\mu C\,cm_{Pt}^{-2}$ as a conversion factor for Pt/VC and Pt_3Co/VC films, respectively.

2.3. SO_2 poisoning experiments in electrochemical cell

Thin-film electrodes with platinum loading of 35 and 20 $\mu g_{Pt}\,cm^{-2}$ for 30 wt.% Pt_3Co/VC and 50 wt.% Pt/VC respectively, were electrochemically cleaned in O_2-free 0.1 M $HClO_4$. Following that, two CVs at 20 mV s^{-1} were recorded using the Autolab potentiostat. Then the electrode potential was set to 0.60 V and current vs. time was recorded in O_2-free atmosphere for the first 5 min. Then 5 ppm SO_2 in UHP N_2 was introduced for 15 min at a flow rate of 20 sccm, followed by 15 min nitrogen purge to remove dissolved SO_2. Finally, ten consecutive CV curves were recorded according to the program: 0.6 V → 0.05 V → 1.4 V → 0.05 V.

All potentials measured in the electrochemical cell are given with respect to a RHE in 0.1 M $HClO_4$.

2.4. Fuel cell testing

Experiments were performed on catalyst coated membranes (CCMs) purchased from Ion Power, Inc. The Pt/VC catalyst coated membranes had a 50 wt.% Pt/VC as the cathode and anode catalysts with a platinum loading of 0.4 $mg_{Pt}\,cm^{-2}$ on both sides of NRE 212 (DuPont) membranes; catalyst-coated areas were 10 cm^2. 50 wt.% Pt/VC catalyst was from the same batch as was used for RDE experiments.

The Pt_3Co/VC CCMs were custom-made for this project by Ion Power, Inc., using the same 30 wt.% (total metal loading) Pt_3Co/VC cathode catalyst (BASF, developmental), as was used in RDE experiments. The Pt loading at these cathodes was also 0.4 $mg_{Pt}\,cm^{-2}$.

CCMs were sandwiched between two gas diffusion layers (SGL 25BC, 236 μm) and mounted into the 10 cm^2 fuel cell test fixture with single-serpentine flow fields (Fuel Cell Technologies). A 890C fuel cell test station with built in current-interrupt capability (Scribner Associates, Inc.) was used for evaluation of the fuel cells.

The effect of SO_2 was tested by introducing 1 ppm SO_2 into the air feed for 3 h at a cell voltage of 0.6 V, at 80 °C and 100% relative humidity. Details of the experiments and "break-in" procedure can be found elsewhere [7,17]. Briefly, ultrahigh purity (UHP) hydrogen (GTS-Welco) and 1 ppm SO_2 in ultrazero (neat) air were flowed through the anode|cathode at flow rates of 0.25|0.5 SLPM while holding the cell voltage at 0.6 V. Before and after exposure to the SO_2–air mixture, the cathode was run in air at a cell voltage of 0.6 V for 2 and 10 h, respectively. After a final air purge, either a set of 10 polarization curves were measured at a stoic ratio $s = 2/2$, or air flow was replaced by nitrogen flow at 0.1 SLPM and hydrogen crossover i_x was measured at $H_2|N_2$ flow rates of 0.25|0.1 SLPM at 80 °C and a scan rate of 1 mV s^{-1} between 0.1 and 0.40 V [18] using an Autolab potentiostat (PGSTAT30). The procedure for measuring polarization curves was adopted from Ref. [19]: current vs. time was recorded at every given cell voltage for 15 min, with the final current value taken from the average of the last 5 min. After measuring polarization curves, the air flow was replaced by nitrogen flow, and hydrogen crossover was determined as it is described above. Then the cell was cooled down to 30 °C, and a set of CV curves were recorded at a scan rate of 50 mV s^{-1} between 0.085 and 1.4 V at $H_2|N_2$ flow rates of 0.25|0.03 SLPM using an Autolab potentiostat. CVs were measured under flooded conditions [19]: humidifiers temperatures were set to 50 °C while the cell was cooled down from 80 to 30 °C. Then the fuel cell was disassembled, and a new CCM was tested. Every contaminated CCM was tested just once and never used again.

If the hydrogen crossover was measured after SO_2 poisoning at 80 °C, the cell was further used to estimate the coverage of sulfur species on the platinum surface from a set of CVs measured at 30 °C. The same protocol for measuring CVs as described above was applied. After running CVs, the cell was heated back to 80 °C, and two more polarization curves in $H_2|$air were recorded. Then the cell was cooled down and disassembled.

For SO_2 contamination experiments in $H_2|N_2$, 30 wt.% Pt_3Co/VC and 50 wt.% Pt/VC cathodes were exposed to 1 ppm SO_2 in UHP nitrogen (GTS-Welco) for 3 h while holding the cathodes at 0.6 and 0.5 V, respectively. Flow rates (0.25|0.5 SLPM at the anode|cathode), cell temperature (80 °C) and relative humidity (100%) were the same as in the $H_2|$air contamination experiments. Potentials in $H_2|N_2$ experiments were applied using the Autolab potentiostat. Before and after exposure to SO_2 in nitrogen, the cathodes were held in nitrogen at 0.6 V for 1 h. After SO_2/N_2 poisoning at 80 °C, the cells were cooled down to 30 °C, and a set of CV curves were recorded under flooded conditions.

The platinum ECSAs for the clean catalysts were determined from the hydrogen desorption region on CV curves measured at 30 °C after the "break-in" procedure preceding SO_2 exposure. The area under the hydrogen desorption peaks were integrated after double-layer correction, i.e. subtracting the currents measured at 0.4 V from the total currents. 200 $\mu C\,cm^{-2}$ [10] and 210 $\mu C\,cm^{-2}$ [9] were used to convert the charge consumed for hydrogen electrochemical desorption into the platinum ECSAs for the 30 wt.% Pt_3Co/VC and 50 wt.% Pt/VC cathodes, respectively.

Every experiment in $H_2|$air or $H_2|N_2$ cells was repeated at least twice to ensure that reproducible results were obtained. All potentials in the FC experiments are given with respect to the potential at the anode.

2.5. X-ray diffraction (XRD)

XRD (Bruker D8 Advance diffractometer [Cu Kα radiation: 40 kV, 40 mA; 1.2° $2\theta\,min^{-1}$ step size]) was used to determine the Pt nanoparticle size for the 30 wt.% Pt_3Co/VC, 20 wt.% Pt/VC and 50 wt.% Pt/VC catalysts. The average Pt nanoparticle diameter was determined by Scherer's equation from the peak observed at $2\theta = 40°$. This approach has been validated with transmission electron microscopy in our previous paper [20].

2.6. TPD

All TPD experiments were performed using a Micromeritics ASAP 2010 chemisorption instrument equipped with a Pfeiffer Vacuum ThermoStar™ mass spectrometer (MS) attachment. 60 mg of a powder catalyst was placed in quartz U-tubes, on-top of a bed of quartz wool. The instrument thermocouple was placed in the powder sample for accurate temperature measurement.

Three powder catalyst samples were analyzed for their SO_2 desorption characteristics: 40 wt.% Pt/VC from Johnson-Matthey, 30 wt.% Pt_3Co/VC (BASF), and acid-leached 30 wt.% Pt_3Co/VC. The acid leached 30 wt.% Pt_3Co/VC was produced by immersing the catalyst in 0.5 M $HClO_4$ at 80 °C for 1 h followed by filtration to recover the catalyst. The catalyst was leached a second time in 0.5 $HClO_4$ at 80 °C for 1 h and filtered after that. After filtration, the powder was washed with a 100 ml of hot 0.5 M $HClO_4$ followed by 100 ml of nanopure H_2O to remove residual cobalt and acid ions. The powder was then vacuum dried at 25 °C overnight.

Prior to adsorption of SO_2 40 wt.% Pt/VC and untreated 30 wt.% Pt_3Co/VC samples were degassed *in situ* at 350 and 550 °C, respectively, in UHP He (99.999%) to clean the surface of any impurities. The acid leached 30 wt.% Pt_3Co/VC sample was degassed at 110 °C to avoid sintering of nanoparticles. After degassing the samples were cooled to 80 °C and exposed to 5 ppm SO_2 in UHP He (99.999%) for 24 h. After exposure to SO_2 in He the samples were flushed and cooled under He to remove any remaining SO_2. Once a stable

Please cite this article in press as: O.A. Baturina, et al., Insights on the SO_2 poisoning of Pt_3Co/VC and Pt/VC fuel cell catalysts, Electrochim. Acta (2010), doi:10.1016/j.electacta.2010.06.004

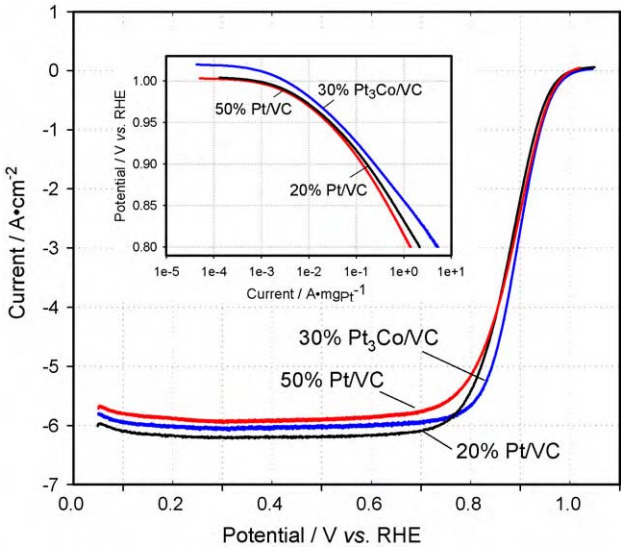

Fig. 1. ORR curves for thin films of 30 wt.% Pt_3Co/VC (20 μg_{Pt} cm^{-2}, blue), 20 wt.% Pt/VC (20 μg_{Pt} cm^{-2}, black) and 50 wt.% Pt/VC (30 μg_{Pt} cm^{-2}, red) recorded during the anodic sweep at 1600 rpm in oxygen-saturated 0.1 M $HClO_4$ at a scan rate of 5 mV s^{-1} at ambient temperature. Current densities per geometric surface area. Inset shows *E* vs. mass-normalized kinetic currents extracted from the ORR curves according to Eq. (1). (For interpretation of the references to color in this figure legend, the reader is referred to the web version of this article.)

baseline was established, the samples were ramped from ambient temperature (~45 °C) to 600 °C at 10 °C min^{-1} in He. During ramping the quartz tube effluent was monitored by the MS and a thermal conductivity detector. The MS was used to monitor the following molecular ions during desorption: H_2O^+(*m*/*e* = 18), CO^+(*m*/*e* = 28), CO_2^+ (*m*/*e* = 44), SO_2^+(*m*/*e* = 64), and SO_3^+(*m*/*e* = 80). Fresh samples were used for each experiment and repeats.

3. Results and discussion

3.1. Characterization of Pt_3Co/VC and Pt/VC catalysts in an electrochemical cell

The RDE results are shown in Fig. 1 for the ORR activity of the 30 wt.% Pt_3Co/VC (blue), 20 wt.% Pt/VC (black) and 50 wt.% Pt/VC (red). Both 30 wt.% Pt_3Co/VC and 20 wt.% Pt/VC have the same platinum loading of 20 μg_{Pt} cm^{-2} whereas platinum loading of 50 wt.% Pt/VC is 30 μg_{Pt} cm^{-2}. The 30 wt.% Pt_3Co/VC and 50 wt.% Pt/VC have significantly different particle sizes (4.3 ± 0.3 and 2.9 ± 0.5 nm, respectively), so the curve for 20 wt.% Pt/VC with particle size of 3.5 ± 0.5 nm is given as a reference. As described in our earlier work [1] and by others [21–25], the curve for the 30 wt.% Pt_3Co/VC is shifted toward more positive potentials vs. 20 wt.% Pt/VC in the mixed kinetic diffusion control region (0.82–1.0 V), indicative of higher mass activity for the Pt_3Co/VC. In spite of a higher platinum loading, the 50 wt.% Pt/VC curve is almost undistinguishable from that of the 20 wt.% Pt/VC catalyst in the potential range of 0.85–1.0 V, meaning lower mass activity for the former catalyst. The reason for this can be a Pt particle size effect, as area-specific activity decreases with the particle size [8,26]. The difference in mass activities of three catalysts can be clearly seen from the inset in Fig. 1.

The voltammetric curves used to determine the platinum ECSAs of the three catalysts by the three different methods described in the experimental section are shown in Figs. 2–4. The platinum loading for all three catalysts was 20 μg_{Pt} cm^{-2}. The difference between CVs measured on 20 wt.% Pt/VC (black) and 30 wt.% Pt_3Co/VC (blue) catalysts in O_2-free 0.1 M $HClO_4$ solution (Fig. 2) has already been

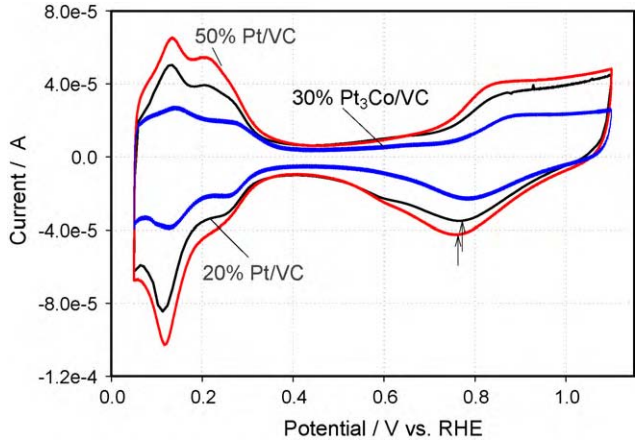

Fig. 2. Cyclic voltammogramms of thin films of 30 wt.% Pt_3Co/VC (blue), 20 wt.% Pt/VC (black) and 50 wt.% Pt/VC (red) catalysts in O_2-free 0.1 M $HClO_4$ solution recorded at 20 mV s^{-1}. Platinum loading 20 μg_{Pt} cm^{-2}, ambient temperature. Arrows indicate peaks at 0.76 and 0.77 V for reduction of oxygen species at 50 and 20 wt.% Pt/VC, respectively. (For interpretation of the references to color in this figure legend, the reader is referred to the web version of this article.)

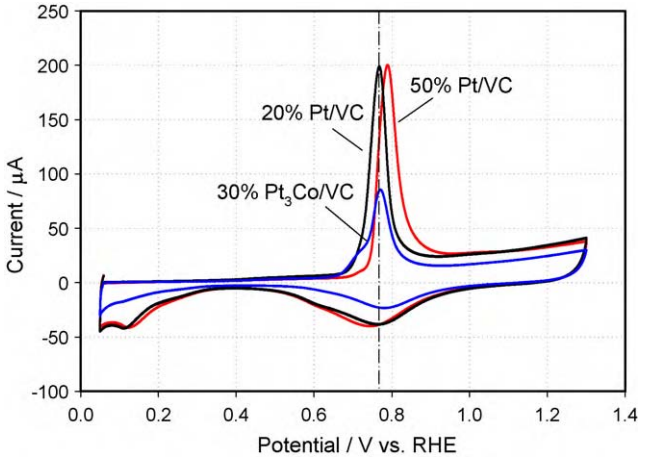

Fig. 3. CO stripping voltammograms of thin film of 30 wt.% Pt_3Co/VC (blue), 20 wt.% Pt/VC (black) and 50 wt.% Pt/VC (red) in O_2-free 0.1 M $HClO_4$ solution recorded at 10 mV s^{-1}. Platinum loading 20 μg_{Pt} cm^{-2}, ambient temperature. Dashed line indicates peaks for CO oxidation on 20 wt.% Pt/VC and 30 wt.% Pt_3Co/VC thin films at 0.77 V. (For interpretation of the references to color in this figure legend, the reader is referred to the web version of this article.)

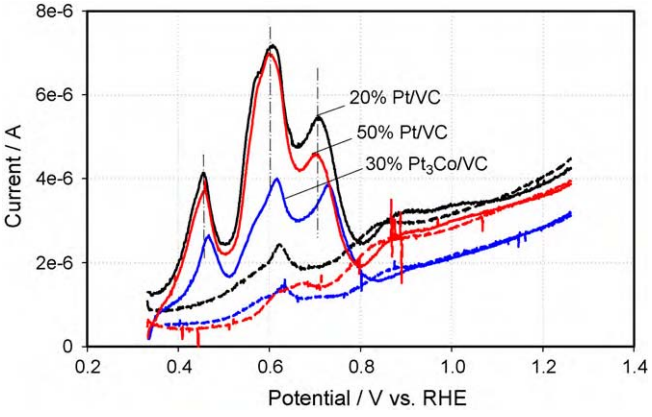

Fig. 4. Cu-*upd* of thin films of 30 wt.% Pt_3Co/VC (blue), 20 wt.% Pt/VC (black) and 50 wt.% Pt/VC (red) in O_2-free 0.1 M $HClO_4$ (dashed lines) and 0.1 M $HClO_4$ + 5 × 10^{-3} M $CuSO_4$ (solid lines). Scan rate 1 mV s^{-1}, platinum loading 20 μg_{Pt} cm^{-2}, ambient temperature. Dashed lines indicate peaks for oxidation of copper adatoms from 20 wt.% Pt/VC and 50 wt.% Pt/VC thin films at 0.46, 0.6 and 0.7 V. (For interpretation of the references to color in this figure legend, the reader is referred to the web version of this article.)

Please cite this article in press as: O.A. Baturina, et al., Insights on the SO_2 poisoning of Pt_3Co/VC and Pt/VC fuel cell catalysts, Electrochim. Acta (2010), doi:10.1016/j.electacta.2010.06.004

Table 1
Platinum ECSAs determined by H-adsorption, CO stripping and Cu-*upd* for thin films of 30 wt.% Pt_3Co/VC, 20 and 50 wt.% Pt/VC: 20 $\mu g_{Pt}\ cm^{-2}$, 0.1 M $HClO_4$, 25 °C.

Catalyst	Pt particle size by XRD (nm)	d_{Pt}/d_{Pt_3Co}	ECSA ($m^2\ g_{Pt}^{-1}$)			$ECSA_{Pt_3Co/VC}/ECSA_{Pt/VC}$		
			H-ad	CO	Cu-*upd*	H-ad	CO	Cu-*upd*
30% Pt_3Co/VC, BASF	4.3 ± 0.3	–	36 ± 2	40 ± 2	45 ± 2	–	–	–
20% Pt/VC, E-TEK	3.5 ± 0.3	0.83 ± 0.1	62 ± 3	65 ± 3	67 ± 3	0.58 ± 0.03	0.62 ± 0.03	0.67 ± 0.03
50% Pt/VC[a]	2.9 ± 0.5	0.67 ± 0.1	70 ± 4	72 ± 4	72 ± 4	0.51 ± 0.03	0.56 ± 0.03	0.63 ± 0.03

[a] Purchased from Ion Power, Inc. Information about manufacturer is not disclosed.

discussed in our previous paper [1]. The CV curve for 50 wt.% Pt/VC (red) has the same features as the one for 20 wt.% Pt/VC. Two differences that are worth mentioning when comparing the two Pt/VC catalysts are higher areas under the hydrogen adsorption/desorption peaks and a ~10 mV negative shift in the peak for reduction of adsorbed oxygen species for 50 wt.% Pt/VC; both are likely due to smaller Pt nanoparticle size for the 50% Pt/VC.

The CO stripping voltammograms (Fig. 3) are characterized by oxidation peaks at 0.77 V for 30 wt.% Pt_3Co/VC (blue) and 20 wt.% Pt/VC (black) and 0.79 V for 50 wt.% Pt/VC (red). The same peak position for 30 wt.% Pt_3Co/VC and 20 wt.% Pt/VC catalysts is indirect evidence of enrichment of the alloy surface with platinum [27]. If cobalt was present on the surface, the alloy would facilitate CO oxidation according to a bifunctional mechanism, and the peak would be shifted negatively relative to the 20 wt.% Pt/VC catalyst.

The CO oxidation peaks for both Pt/VC catalysts are well pronounced, sharp single peaks, while the peak for the 30 wt.% Pt_3Co/VC has a well defined shoulder at 0.67–0.74 V. The shape of the shoulder is not always reproducible, which does not affect the area under the peak, though. The presence of two contributions to CO electrooxidation peak on carbon-supported $Pt_{85}Co_{15}$ alloy was also reported by Garcia et al. [28]. Although the nature of the second contribution is unclear, some factors such as the presence of a significant amount of bridge-bonded CO can be eliminated [28]. The shoulder is likely related to the formation of irregularities on the alloy surface during the formation of a platinum "skeleton" [10,29] or enrichment of the Pt_3Co surface layer with platinum atoms [10,29].

The negative shift in the CO oxidation peak (Fig. 3) for 20 wt.% Pt/VC vs. 50 wt.% Pt/VC with increasing particle size (3.5 ± 0.5 vs. 2.9 ± 0.5 nm, respectively) is consistent with the particle size effect on CO monolayer oxidation reported by Maillard et al. [30]. The area under the CO oxidation peak is remarkably smaller for the Pt_3Co/VC catalyst indicative of a smaller platinum ECSA. Due to the unusual shape of the CO oxidation peak of the alloy catalyst and associated with it uncertainties in Pt ECSA determination, the Cu-*upd* method was implemented as an additional method to evaluate the ECSA of three catalysts. Voltammetric curves for oxidation of Cu adatoms from thin films of 30 wt.% Pt_3Co/VC (blue) 20 wt.% Pt/VC (black) and 50 wt.% Pt/VC (red) are illustrated in Fig. 4. Background curves measured in the absence of copper adatoms are shown as a reference. The small, but distinguishable features on the background curves in the potential range of 0.5–0.7 V result from trace impurities present in the electrolyte that produce more pronounced effect at low scan rates. Cu oxidation curves are characterized by three oxidation peaks at 0.46, 0.6 and 0.7 V for Pt/VC catalysts and 0.47, 0.62 and 0.73 V for Pt_3Co/VC. These peaks are assigned to copper sites of different adsorption energies [31]. The positive shift in peak positions for Pt_3Co/VC vs. Pt/VC probably indicates that the Cu adatoms have higher adsorption energies on Pt alloy nanoparticles then on pure platinum nanoparticles

Platinum ECSAs determined by H-adsorption, CO stripping and Cu-*upd* are compared in Table 1. ECSAs determined by three different methods for Pt/VC catalysts are consistent within 10 ± 5% error, while higher discrepancy is observed for P_3Co/VC catalyst. The differences between ECSAs obtained by H-adsortpion (36 ± 2 m^2/g_{Pt}) vs. CO stripping (40 ± 2 m^2/g_{Pt}) and Cu-*upd* (45 ± 2 m^2/g_{Pt}) for the alloy catalyst are 11 ± 5 and 25 ± 5%, respectively. Since CO stripping and Cu-*upd* are considered more reliable techniques for ECSA determination and there is a reasonable (~10%) agreement between two ECSAs values, we assume that these values represent platinum surface area of Pt_3Co/VC catalyst. The next important question is whether the difference between the platinum ECSAs for Pt_3Co/VC and Pt/VC catalysts is only due to different Pt particle sizes or also due to the presence of cobalt on the surface of the alloy. In order to answer this question, the ratio of diameters of platinum and alloy nanoparticles (d_{Pt} and d_{Pt_3Co}, respectively) is compared to the ratio of platinum ECSAs for the Pt_3Co/VC and Pt/VC catalysts for each method of ECSA evaluation. Using approximation that platinum ECSA is inversely proportional to the diameter of the nanoparticle d [32], the ratio of ECSAs for two catalysts having only platinum atoms on the surface of the nanoparticles can be estimated according to Eq. (2):

$$\frac{ECSA_{Pt_3Co/VC}}{ECSA_{Pt/VC}} = \frac{\rho_{Pt} d_{Pt}}{\rho_{Pt_3Co} d_{Pt_3Co}} \quad (2)$$

where ρ_{Pt_3Co} and ρ_{Pt} are Pt_3Co and Pt densities, respectively. For example, for 4.3 nm Pt_3Co nanoparticles and 3.5 nm Pt nanoparticles, the lower limit for the right part of Eq. (2) is 3.5/4.3 nm = 0.81. In fact, the real value is greater than 0.81, as the ratio of densities of Pt and Pt_3Co is greater than one. The criterion for the cobalt presence on the surface is the lower value of the left part of Eq. (2) compared to the right one. The ratios of diameters of Pt and Pt_3Co nanoparticles and ECSAs of Pt_3Co/VC and Pt/VC catalysts for all three catalysts are given in Table 1 (Columns 3, 7–9). The closest agreement (within experimental error) between the left and right parts of Eq. (2) is obtained for ECSAs of 30 wt.% Pt_3Co/VC and 50 wt.% Pt/VC catalysts estimated by the Cu-*upd* method (0.63 ± 0.03 and 0.67 ± 0.10, respectively). For the 20 wt.% Pt/VC catalyst, the difference is greater (0.67 ± 0.03 vs. 0.81 ± 0.10) which probably reflects larger uncertainties in particle size determination for this catalyst. Thus, we assume below that the difference in the Pt ECSAs of Pt_3Co/VC and Pt/VC catalysts is due to the different particle size of these catalysts, and either a Pt "skeleton" [10] or platinum-enriched layer [29] is formed on the surface of Pt_3Co nanoparticles under acidic conditions.

However, ECSAs determined by H-adsorption are used in the analysis of the area-specific activities for the ORR that follows. Since H-adsorption is still the easiest way to measure platinum ECSA both in an electrochemical cell and in a fuel cell, the majority of researchers report area-specific activities for ORR based on the H-adsorption region on CV curves. All proceeding platinum ECSA measurements will be from the H-adsorption region in order to compare our results with the existing literature.

Mass- and area-specific activities for Pt_3Co/VC and Pt/VC catalysts are given in Table 2. The mass activity of the Pt_3Co/VC catalyst is lower (0.24 ± 0.02 A mg_{Pt}^{-1}) than reported previously by our group (0.30 ± 0.03 A mg_{Pt}^{-1}) [1] because a different batch of developmental catalyst was used in this study. The area-specific activity of the 30 wt.% Pt_3Co/VC catalyst towards the ORR (670 ± 60 μA cm_{Pt}^{-2}) is 2.5 times higher than that of 20 wt.% Pt/VC (270 ± 30, 670 ± 60 μA cm_{Pt}^{-2}), while its mass-specific activ-

Please cite this article in press as: O.A. Baturina, et al., Insights on the SO_2 poisoning of Pt_3Co/VC and Pt/VC fuel cell catalysts, Electrochim. Acta (2010), doi:10.1016/j.electacta.2010.06.004

Table 2
Mass-specific (A mg_{Pt}^{-1}) and area-specific ($\mu A\,cm_{Pt}^{-2}$) activities for the ORR at 0.9 V in 0.1 M $HClO_4$: 1600 rpm, 5 mV s^{-1}, 25 °C.

Catalyst	Pt loading ($\mu g_{Pt}\,cm^{-2}$)	A mg_{Pt}^{-1} (±10%)	$\mu A\,cm_{Pt}^{-2}$ (±10%)
30% Pt_3Co/VC	20 ± 0.25	0.24	670
20% Pt/VC	20 ± 0.25	0.17	270
50% Pt/VC	30 ± 0.25	0.12	170

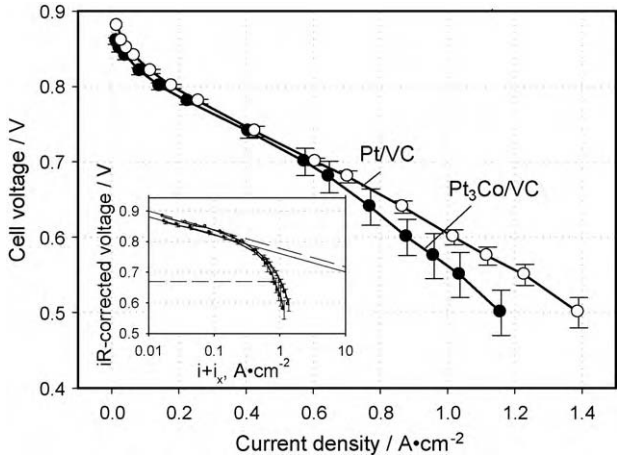

Fig. 5. Polarization curves measured on single cells employing 30 wt.% Pt_3Co/VC (solid circles) and 50 wt.% Pt/VC (open circles) at the cathodes. Platinum loading 0.4 $mg_{Pt}\,cm^{-2}$, 80 °C, 100% RH. Insert shows polarization curves in Tafel coordinates. Dashed horizontal line corresponds to cell voltage of 0.6 V.

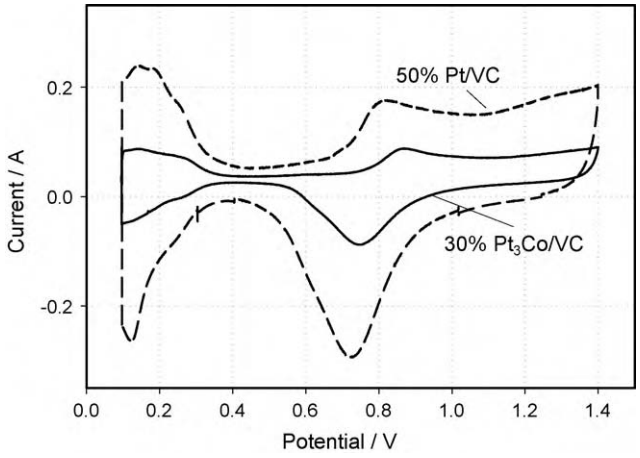

Fig. 6. Cyclic voltammograms measured under $H_2|N_2$ in single cells employing 30 wt.% Pt_3Co/VC (solid) and 50 wt.% Pt/VC (dashed line) at the cathodes. Scan rate is 50 mV s^{-1}, cell and humidifiers temperatures are 30 and 50 °C, respectively. Platinum loading is 0.4 $mg_{Pt}\,cm^{-2}$ and $H_2|N_2$ flow rates are 0.25|0.03 L min^{-1}.

ity (0.24 ± 0.02 A mg_{Pt}^{-1}) is only 1.5 times higher than that of 20 wt.% Pt/VC (0.17 ± 0.02 A mg_{Pt}^{-1}). The area-specific activity of 30 wt.% Pt_3Co/VC (670 ± 60 $\mu A\,cm_{Pt}^{-2}$) is consistent with those reported by other researchers [21,23–25]. The 50 wt.% Pt/VC has the lowest mass- and area-specific activities (0.12 ± 0.01 A mg_{Pt}^{-1} and 170 ± 20 $\mu A\,cm_{Pt}^{-2}$, respectively) of the three catalysts.

3.2. Fuel cell testing

3.2.1. Fuel cell performance in H_2|air

Polarization curves measured in H_2|air single cells employing 30 wt.% Pt_3Co/VC (custom-made CCMs) and 50 wt.% Pt/VC catalysts (commercial CCMs) at the cathodes are illustrated in Fig. 5. Interestingly, the 50 wt.% Pt/VC demonstrates higher performance than the 30 wt.% Pt_3Co/VC over the whole range of current densities. This is inconsistent with the higher mass-specific activity observed for the 30 wt.% Pt_3Co/VC using the RDE technique (see Fig. 1). To understand the reason behind such disagreement, polarization curves were measured in $H_2|O_2$ single cells at the same conditions as in H_2|air fuel cells (except for s = 2/10 vs. 2/2), and mass- and area-specific activities toward the ORR were calculated for the 30 wt.% Pt_3Co/VC and 50 wt.% Pt/VC catalysts from ohmic resistence (R)-corrected polarization curves at iR-corrected voltage of 0.9 V (Table 3). For the reason discussed above, area-specific activities are given with respect to ECSAs evaluated from the H-adsorption region of the CVs measured in $H_2|N_2$ cells (see Fig. 6). Both area- and mass-specific activities are normalized to an O_2 partial pressure of 100 kPa_{abs} according to Eq. (18) in Ref. [19] assuming that the ORR is a first-order reaction with respect to oxygen partial pressure. Using this normalization, we are able not only to compare the catalyst activities in fuel cell experiments to those reported by others [8], but also to compare activities in fuel cells to those in electrochemical cells. Although it is accepted in the literature [8] to compare RDE activities at 60 °C to fuel cell activities at 80 °C, we do not find significant difference between RDE activities measured at 30 and 60 °C for initial catalyst evaluation [33]. Therefore, RDE activities measured at room temperature will be compared below to fuel cell activities in $H_2|O_2$ cells measured at 80 °C.

Area-specific normalized activity of the 50 wt.% Pt/VC in the fuel cell (150 ± 20 $\mu A\,cm_{Pt}^{-2}$) is in agreement with the value obtained in the electrochemical cell (170 ± 20 $\mu A\,cm_{Pt}^{-2}$), but 20–30% lower than the activity reported by Gasteiger et al. [8] (180–210 $\mu A\,cm_{Pt}^{-2}$) for a ~50 wt.% Pt/C catalysts from TKK. Unlike the 50 wt.% Pt/VC, area-specific activity of the 30 wt.% Pt_3Co/VC in the fuel cell (390 ± 20 $\mu A\,cm_{Pt}^{-2}$) is 1.7 times lower than that in the electrochemical cell (670 ± 20 $\mu A\,cm_{Pt}^{-2}$). This can be due to a combination of several reasons. First, the catalyst ink for Pt_3Co/VC was not optimized, as the same platinum/ionomer ratio was used for both catalysts. One of the indicators of a non-optimized ink is that not all the platinum surface is accessible for oxygen adsorption (not utilized). The lower platinum utilization seen for cathodes with 30 wt.% Pt_3Co/VC vs. 50 wt.% Pt/VC (69 vs. 97%, respectively, Table 4) directly confirms this fact. Platinum utilization is defined here as the ratio of platinum ECSA measured in an electrochemical cell to platinum ECSA measured in a fuel cell for a given catalyst [19]. Second, cobalt leaching from the Pt_3Co/VC catalyst can replace some of protons in the Nafion ionomer surrounding the catalyst [8] which are essential for the ORR to occur. It might have

Table 3
Mass-specific and area-specific activities for the ORR at iR-corrected voltage of 0.9 V in $H_2|O_2$ single cell at s = 2/10, 80 °C, 100% RH and ambient pressure.

Catalyst	Pt loading ($mg_{Pt}\,cm^{-2}$)	ECSA ($m^2\,g_{Pt}^{-1}$)	A mg_{Pt}^{-1} (±10%)	A mg_{Pt}^{-1} [a] (±10%)	$\mu A\,cm_{Pt}^{-2}$ (±10%)	$\mu A\,cm_{Pt}^{-2}$ [a] (±10%)
30% Pt_3Co/VC	0.4 ± 0.02	25 ± 2	0.05	0.09	210	390
50% Pt/VC	0.4 ± 0.02	68 ± 5	0.06	0.10	80	150

[a] Activities normalized to O_2 partial pressure of 101.3 kPa at the cathode.

Please cite this article in press as: O.A. Baturina, et al., Insights on the SO_2 poisoning of Pt_3Co/VC and Pt/VC fuel cell catalysts, Electrochim. Acta (2010), doi:10.1016/j.electacta.2010.06.004

Table 4
Platinum ECSA measured in $H_2|N_2$ single cells at 30 °C (cell) and 50 °C (humidifiers) and Pt utilization of 30 wt.% Pt_3Co/VC and 50 wt.% Pt/VC.

Catalyst	Pt loading ($mg_{Pt}\,cm^{-2}$)	ECSA ($m^2\,g_{Pt}^{-1}$)	Pt utilization (%)
30% Pt_3Co/VC	0.4 ± 0.02	25 ± 2	69
50% Pt/VC	0.4 ± 0.02	68 ± 5	97

two consequences: first, the ORR can become less efficient and second, the cell resistance can increase as a result of the replacement of protons by cobalt ions. However, the later effect is taken into account by the area-specific activity calculations at an *iR*-free cell voltage.

The area-specific activity of Pt_3Co/VC-cathodes in the FC is lower than that measured in the electrochemical cell, but still 2.6 times higher than the activity of Pt/VC. Also, it is only 30% lower than 550 $\mu A\,cm_{Pt}^{-2}$ reported for Pt_xCo_{1-x}/C catalyst from TKK [9]. Note, that even though the Pt particle sizes are different for 30 wt.% Pt_3Co/VC and 50 wt.% Pt/VC catalysts, a factor of two increase in area-specific activity cannot be justified only by a particle size effect. Particle size effect would result in 20–30% increase in area-specific activity for 4.3 vs. 2.9 nm platinum nanoparticles [9,22].

The normalized mass-specific activities of 30 wt.% Pt_3Co/VC ($0.09 \pm 0.01\,A\,mg_{Pt}^{-1}$) and 50 wt.% Pt/VC ($0.1 \pm 0.01\,A\,mg_{Pt}^{-1}$) are approximately the same and close to the mass activity of $0.11\,A\,mg_{Pt}^{-1}$ reported in Ref. [8] for a 47% Pt/C with a similar platinum ECSA of 70 m^2/g_{Pt}. A factor of two lower mass-specific activity of the 30 wt.% Pt_3Co/VC catalyst compared to the benchmark TKK catalyst ($0.28\,A\,mg_{Pt}^{-1}$) is mostly due to a lower platinum ECSA of the former catalyst (25 vs. 50 $m^2\,g_{Pt}^{-1}$).

The CVs used for the platinum ECSA calculation in fuel cell experiments are shown in Fig. 6. They have the same features as the ones measured in the 3-electrode electrochemical cell (see Fig. 2). In terms of current densities, the difference between the CVs measured for Pt_3Co/VC-cathodes and Pt/VC cathodes is even more pronounced in the fuel cell vs. the electrochemical cell, leading to a greater difference between ECSAs (25 ± 3 vs. $68 \pm 5\,m^2\,g_{Pt}^{-1}$, respectively).

3.2.2. SO_2 poisoning experiments in fuel cells

The influence of SO_2 on the performance of PEM fuel cells employing the 30 wt.% Pt_3Co/VC and 50 wt.% Pt/VC was studied by introduction of 1 ppm SO_2 in air at a voltage of 0.6 V, and the results are presented in Fig. 7. Both cathodes exhibit significant performance degradation during exposure to SO_2. The current density decreases by 86 and 49% for cathodes employing 30 wt.% Pt_3Co/VC and 50 wt.% Pt/VC, respectively. Partial performance recovery is observed after replacing the flow of 1 ppm SO_2 in air with a flow of neat air; the current increases by 19 and 7% after 10 h of purging with neat air for cathodes employing 30 wt.% Pt_3Co/VC and 50 wt.% Pt/VC, respectively. At first glance, the alloy cathodes seem more susceptive to SO_2 poisoning. However, the two catalysts have remarkably different ECSAs, and exposure of the catalyst with lower surface area to the same dosage of SO_2 is equivalent to exposure of the same ECSA to a higher dosage of SO_2. To account for the surface area effect, currents measured on fuel cells with 30 wt.% Pt_3Co/VC and 50 wt.% Pt/VC were normalized to ECSAs, determined from H-desorption region on cyclic voltammetry curves (insert to Fig. 7). In the beginning, before SO_2 was introduced to the cathodes (t = 0–2 h in Fig. 7), the ORR current was under mixed kinetic-diffusion control, with a major contribution from diffusion. It is clearly seen from Tafel plots shown in the inset to Fig. 5, considering that the cell voltage of 0.6 V corresponds to *iR*-corrected voltage of 0.66–0.67 V for both catalysts. An interesting feature of the insert in Fig. 7 is that at $t \sim 4$ h, the ECSAs-normalized currents for the two catalysts approach each other. It means probably that on a SO_2-covered surface, the ORR becomes kinetically controlled, with the same reaction rate for both catalysts.

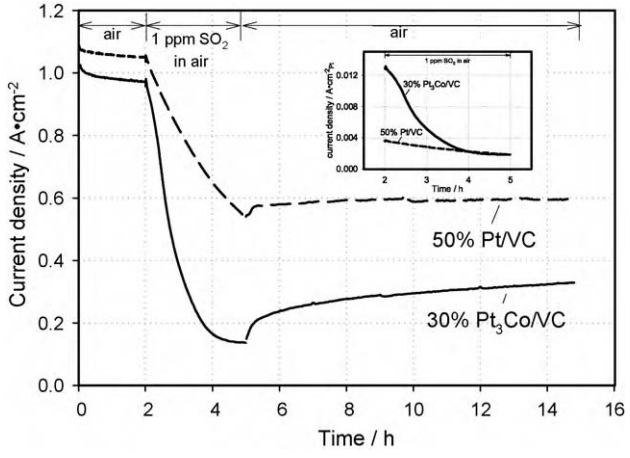

Fig. 7. Current density vs. time at cell voltage of 0.60 V for SO_2 contamination at the cathodes employing 30 wt.% Pt_3Co/VC (solid line) and 50 wt.% Pt/VC (dashed line). Exposure to 1 ppm SO_2 in air was preceded and followed by exposure to neat air for 1 and 10 h, respectively. Inset shows current normalized to platinum ECSA vs. time for the same catalysts. Pt loading 0.4 $mg_{Pt}\,cm^{-2}$, 80 °C, 100% RH.

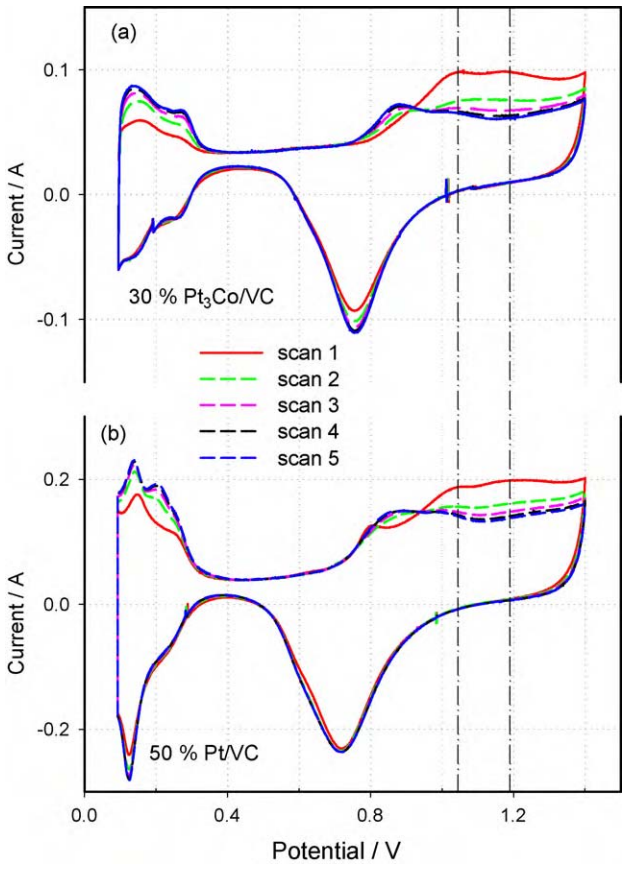

Fig. 8. Five consecutive CVs recorded at 50 mV s^{-1} after exposure of the 30 wt.% Pt_3Co/VC (a) and 50 wt.% Pt/VC (b) cathodes to 1 ppm SO_2 at a cell voltage of 0.60 V. The cell and humidifiers temperatures are 30 and 50 °C. The flow rate is 0.25|0.03 L min^{-1} (anode|cathode). Dashed lines indicate peaks for sulfur oxidation at 1.05 and 1.19 V.

Five successive CVs measured in $H_2|N_2$ cells at 30 °C after SO_2 contamination are shown for Pt_3Co/VC and Pt/VC cathodes in Fig. 8a and b, respectively. The features of the two sets of CVs are similar to each other and have been described in our previous papers [7,17]. Note that both peaks for sulfur oxidation observed during the first

CV sweep at 1.05 and 1.19 V (red curves) are located at the same potentials for both catalysts.

When potential cycling is performed between 0.09 and 1.40 V, adsorbed sulfur is oxidized to sulfate according to the equation proposed by Loucka [34]:

$$Pt - S_{ads} + 4H_2O \rightarrow SO_4^{2-} + 8H^+ + 6e^- + Pt \quad (3)$$

As sulfate does not adsorb on platinum at 1.4 V [35], it leaves the surface, making it available for hydrogen/oxygen adsorption during the next cycle. With progressive scans, more sulfur species are oxidized to sulfate and the CVs acquire a shape that is reminiscent of that of a clean platinum surface. Five successive scans were usually enough to get a reproducible cyclic voltammogram.

The coverage of the platinum surface with sulfur species θ_S after exposure to SO_2 was calculated, for both catalysts, from the hydrogen desorption region on CVs according to Eq. (4):

$$\theta_S = \frac{Q_5 - Q_1}{Q_5} \quad (4)$$

where Q_1 and Q_5 are the charges consumed for hydrogen desorption from contaminated (scan 1) and the clean (scan 5) platinum surface, respectively. Calculating the Pt sulfur coverage using Eq. (4) suggests that one platinum atom adsorbs one sulfur atom. Shortcomings around this assumption have been discussed in our previous paper [7]. The true physical meaning of the sulfur coverage calculated according to Eq. (4) is a fraction of platinum sites not accessible for hydrogen adsorption.

Sulfur coverage calculated from the CV series shown in Fig. 8 is 0.58 ± 0.05 and 0.22 ± 0.02 for 30 wt.% Pt_3Co/VC and 50 wt.% Pt/VC cathodes, respectively. Interestingly, only five scans is required to recover both catalysts even though the sulfur coverage of 30 wt.% Pt_3Co/VC catalyst is a factor of 2.6 higher. The higher sulfur coverage obtained for the 30 wt.% Pt_3Co/VC cathode catalyst suggests that at a given platinum loading (0.4 mg_{Pt} cm^{-2}), the Pt_3Co/VC catalyst is more susceptive to SO_2 poisoning than the Pt/VC. A similar conclusion was made in our previous paper [1] where SO_2 adsorption on thin films of 30 wt.% Pt_3Co/VC and 20 wt.% Pt/VC from electrolyte solution was compared. However, comparing the ECSA-normalized currents shown in insert to Fig. 7 ($t \geq 4$ h), another conclusion important for understanding the fundamental differences between Pt_3Co/VC and Pt/VC catalysts can be made. Even at three times higher sulfur-coverage observed at Pt_3Co/VC cathodes, the ORR currents are the same for both catalysts if ECSA-normalized currents are considered. This implies that if the catalysts with comparable surface areas were investigated, the Pt_3Co/VC catalyst could be less susceptive to SO_2 poisoning.

To evaluate the effect of SO_2 adsorption on the fuel cell's performance, polarization curves were measured on single cells employing 30 wt.% Pt_3Co/VC and 50 wt.% Pt/VC cathode catalysts. Fig. 9 compares polarization curves measured before (black circles) and after (green circles) poisoning of the fuel cell cathodes with 1 ppm SO_2 for 3 h followed by 10 h air purge at 0.60 V. Although significant performance degradation is observed for both fuel cells after exposure to SO_2, it is more pronounced for fuel cell with 30 wt.% Pt_3Co/VC at the cathode (green solid circles), in agreement with the higher sulfur coverage obtained from the CVs.

The insert to Fig. 9 shows the *iR*-corrected voltage vs. hydrogen-crossover-corrected current density in semi-logarithmic coordinates. All the curves have linear regions at current densities lower than 0.1 A cm^{-2}. Within experimental error, the linear region of the polarization curve obtained for the contaminated 50 wt.% Pt/VC has the same slope as the clean 50 wt.% Pt/VC and 30 wt.% Pt_3Co/VC (69 ± 7 mV). This suggests that at low SO_2-coverages (0.22 ± 0.03), SO_2 species block a fraction of the platinum surface making them unavailable for adsorption of oxygen, but do not affect the mechanism of the ORR [7]. Unlike the Pt/VC-contaminated

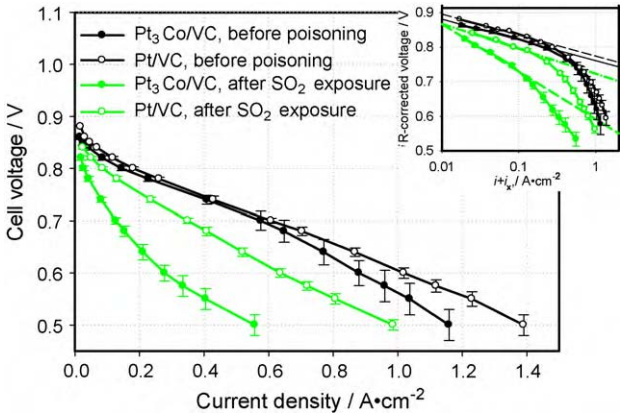

Fig. 9. Polarization curves measured before contamination of the fuel cell cathodes employing 30 wt.% Pt_3Co/VC (black solid circles) and 50 wt.% Pt/VC (black open circles) and after contamination with SO_2 at a cell voltage of 0.6 V (green solid and open circles for 30 wt.% Pt_3Co/VC and 50 wt.% Pt/VC, respectively). Insert shows *iR*-corrected polarization curves in Tafel coordinates. Dashed lines are obtained by linear regression of linear parts of the polarization curves. Platinum loading 0.4 mg_{Pt} cm^{-2}, 80 °C, 100% RH, $s = 2/2$. (For interpretation of the references to color in this figure legend, the reader is referred to the web version of this article.)

surface, the slope of the linear region of the polarization curve measured for the Pt_3Co/VC (137 ± 10 mV) dramatically differs from that of the clean surface. It implies that the mechanism of the ORR depends on the SO_2 coverage, as the coverage observed on the Pt_3Co/VC catalyst (0.58 ± 0.05) was significantly higher than that of the Pt/VC (0.22 ± 0.03). An increase in Tafel slopes (96–110 mV) at a sulfur coverage of 0.42 was also observed in our previous paper [17], where contamination of 50 wt.% Pt/VC cathode with 1 ppm of SO_2, H_2S and COS for 12 h-exposure times was investigated.

As we reported earlier [17], running successive polarization curves results in recovery of the fuel cell's performance. This can be attributed to a decrease of SO_2 coverage due to the oxidation of SO_2 to sulfate with shifting the electrode potential towards the open circuit voltage (OCV) [7]. Fig. 10a and b shows the 1st and the 8th polarization curves measured after contamination of 30 wt.% Pt_3Co/VC (a) and 50 wt.% Pt/VC (b) cathodes with 1 ppm SO_2 in air. Even though the fuel cell with 30 wt.% Pt_3Co/VC cathodes was more severely contaminated after exposure to SO_2 ($\theta_S = 0.58 \pm 0.05$), eight curves were enough for both fuel cells to get reproducible polarization curve, that did not change during successive scans. It implies that 30 wt.% Pt_3Co/VC catalyst can be recovered more easily in air than 50 wt.% Pt/VC. In addition, the potential difference between the linear regions of the polarization curves, measured before poisoning and after running successive polarization curves is larger for the 50 wt.% Pt/VC (15 ± 3 mV) than for the 30 wt.% Pt_3Co/VC (7 ± 3 mV), which suggests more complete recovery for the alloy compared to the platinum catalyst.

Recovery by running successive polarization curves can be interpreted in terms of oxidation of SO_2 to sulfate when the cell voltage progressively changes from 0.5 to 0.9 V. At 0.9 V SO_2 is oxidized to sulfate [7,36], which impedes the ORR [37]. We assume that the shift in potential between the linear regions of the polarization curves given in Fig. 10 is due to the sulfate adsorption on the platinum surface. Sulfate adsorption is weaker on Pt_3Co/VC than on Pt/VC [37], which results in a smaller difference between the linear regions of the polarization curves measured before poisoning and after running eight polarization curves for 30 wt.% Pt_3Co/VC (Fig. 10a) than for 50 wt.% Pt/VC (Fig. 10b).

Recovery by potential cycling occurs faster for the 30 wt.% Pt_3Co/VC fuel cell cathode even though it was more severely contaminated after exposure to SO_2 (Fig. 10a vs. b). In our previous paper [1] we assumed that this is due to the weaker

Please cite this article in press as: O.A. Baturina, et al., Insights on the SO_2 poisoning of Pt_3Co/VC and Pt/VC fuel cell catalysts, Electrochim. Acta (2010), doi:10.1016/j.electacta.2010.06.004

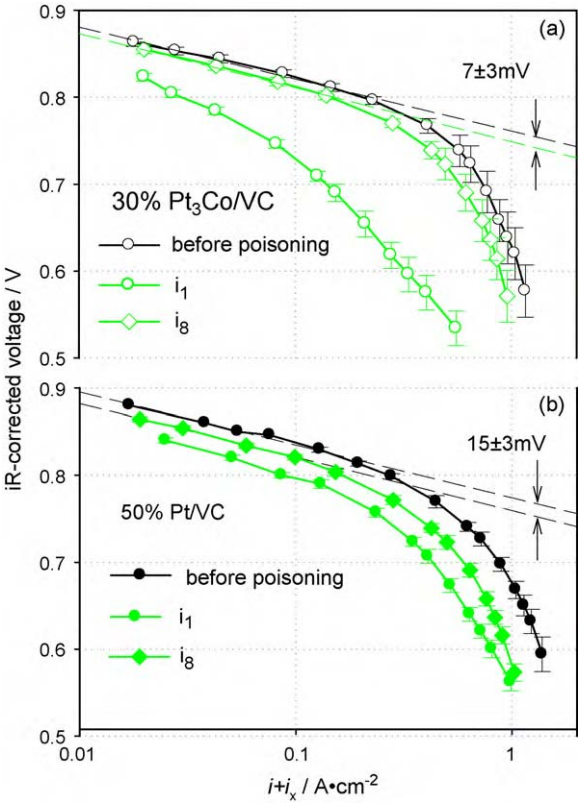

Fig. 10. Polarization curves measured on 30 wt.% Pt_3Co/VC (a, open symbols) and 50 wt.% Pt/VC (b, solid symbols) cathodes before contamination with 1 ppm SO_2 (black circles), after contamination (green circles) and after running eight successive polarization curves (green diamonds). Platinum loading 0.4 mg_{Pt} cm^{-2}, 80 °C, 100% RH, $s = 2/2$. (For interpretation of the references to color in this figure legend, the reader is referred to the web version of this article.)

platinum–sulfur bond in the platinum–cobalt catalyst, indicated by DFT analysis [3]. However, it has not been experimentally proven that platinum–sulfur bond is weaker for Pt_3Co vs. Pt. Second, even if Pt–sulfur bond is weaker for Pt_3Co at a metal/gas interface it does not necessarily mean that (a) it is weaker at a metal/liquid interface and (b) reaction rate of SO_2 oxidation at a metal/liquid interface will be determined by the energetics of the Pt–sulfur bond. The results of some additional experiments are reported below to clarify the differences between Pt_3Co/VC and Pt/VC catalysts in terms of SO_2 adsorption and oxidation.

3.3. Probing SO_2–platinum interaction at catalyst/inert gas interface by TPD

Fig. 11 shows TPD desorption spectra of molecular SO_2 ($m/e = 64$) pre-adsorbed on 30 wt.% Pt_3Co/VC (solid line), acid-treated 30 wt.% Pt_3Co/VC (solid line) and 40 wt.% Pt/VC (dashed line) at 80°C. TPD spectrum for 40 wt.% Pt/VC has one desorption peak at 217 °C. Spectrum of 30 wt.% Pt_3Co/VC is characterized by two peaks: a dominant peak of SO_2 desorption at 203 °C and a broader peak at 380 °C. The first peak is apparently due to SO_2 desorption from platinum: it is in the vicinity of SO_2 desorption peak from Pt/VC catalyst and its intensity is higher than the intensity of the second peak, in agreement with higher atomic ratio of platinum in Pt_3Co alloy. The observed shifting of the SO_2 desorption temperature from 217 to 203 °C is likely an indicator of a weaker platinum–sulfur bond in Pt_3Co/VC catalyst. A similar shift to lower temperatures was reported for CO desorption from Pt(1 1 1) surface vs. $Co_{75}Pt_{25}$ alloy [38]. It was assigned to weakening of the Pt–C bond based on both TPD and Fourier transformed infrared reflection absorption

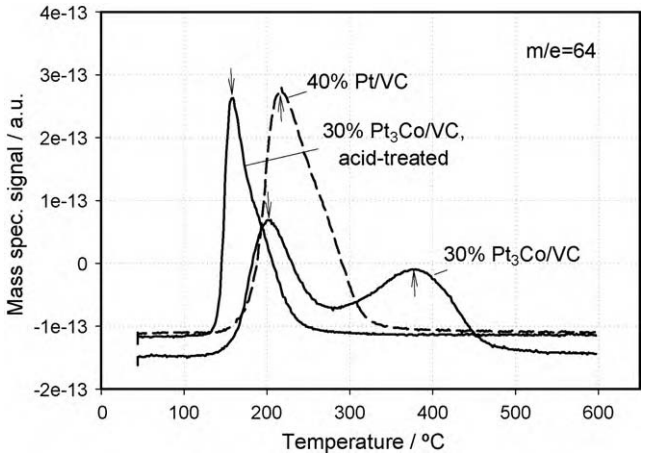

Fig. 11. TPD spectra of pre-adsorbed molecular SO_2 ($m/e = 64$) on 30 wt.% Pt_3Co/VC, acid-treated 30 wt.% Pt_3Co/VC and 40 wt.% Pt/VC recorded in helium. Arrows indicate SO_2 desorption peaks at 203 and 380 °C for 30 wt.% Pt_3Co/VC, 158 °C for acid-treated 30 wt.% Pt_3Co/VC and 217 °C for 40 wt.% Pt/VC.

spectroscopy results. The second peak is most likely due to SO_2 desorption from Co as the Co–S bond is much stronger than Pt–S bond based on DFT analysis [3]. To test this hypothesis, SO_2 desorption spectrum from acid leached 30 wt.% Pt_3Co/VC was measured by TPD (solid line). Obviously, the peak at 380 °C for SO_2 desorption from untreated 30 wt.% Pt_3Co/VC catalyst can be assigned to SO_2 desorption from cobalt, as only one desorption peak at 158 °C is observed for acid-treated alloy catalyst. Shifting of SO_2 desorption peak to lower temperature (158 °C) for acid-treated catalyst suggests weakening of the platinum–sulfur bond after acid-treatment.

Cobalt leaching from the surface of the acid-treated 30 wt.% Pt_3Co/VC catalyst was directly confirmed by inductively coupled plasma-MS analysis of the effluent collected after catalyst's acid treatment. In the first approximation, ~30 wt.% of initial cobalt content found in the effluent can be translated into approximately three cobalt-free monolayers on the surface of 4.3 nm Pt_3Co nanoparticles.

3.4. Probing SO_2–platinum interaction by cyclic voltammetry

In order to account for surface area effects during SO_2 adsorption, Pt/VC and Pt_3Co/VC thin-films electrodes were prepared with the same platinum surface areas by CO and Cu-*upd*. Poisoning was performed at room temperature by purging 0.1 M $HClO_4$ electrolyte with 5 ppm SO_2 in nitrogen for 15 min while holding the electrode potential at 0.6 V. This time was sufficient to get sulfur coverage ~0.8 by Eq. (4). These experimental conditions (except temperature) were close enough to both SO_2 poisoning experiments in H_2|air fuel cells described above and H_2|N_2 cells reported in our previous paper [7].

Series of successive CVs recorded after SO_2 poisoning of 30 wt.% Pt_3Co/VC and 50 wt.% Pt/VC thin films in an electrochemical cell in O_2-free atmosphere are shown in Fig. 12a and b, respectively. The two series of CV curves look surprisingly similar. On the first negative-going scan (0.6 → 0.05 V), a two-wave SO_2 reduction current is observed for both catalysts. On the positive-going scan (0.05 → 1.4 V), a significant suppression of the hydrogen region is observed for both catalysts due to blocking of the platinum surface by sulfur adatoms resulting from SO_2 reduction. Onsets of sulfur oxidation (0.9 V) and peak positions for sulfur oxidation to sulfate (1.2 V) are the same for both catalysts meaning the same adsorption energy for sulfur adatoms at the electrode/solution interface. The first difference between the two catalysts appears when the potential is swept from 1.4 to 0.6 V. The peak position for reduc-

Please cite this article in press as: O.A. Baturina, et al., Insights on the SO_2 poisoning of Pt_3Co/VC and Pt/VC fuel cell catalysts, Electrochim. Acta (2010), doi:10.1016/j.electacta.2010.06.004

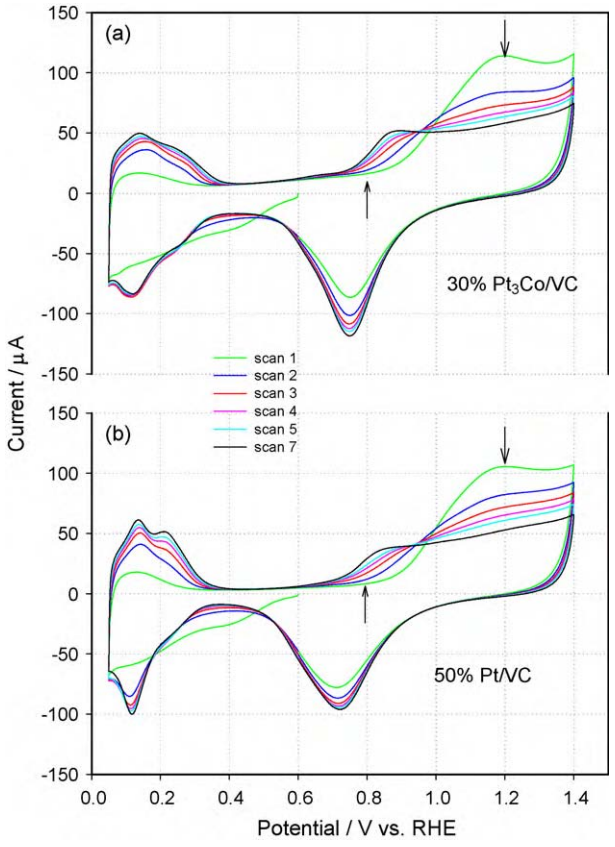

Fig. 12. Seven consecutive CVs recorded after exposure of the 30 wt.% Pt_3Co/VC (a) and 50 wt.% Pt/VC (b) thin-film electrodes to 1 ppm SO_2 in nitrogen for 15 min at 0.6 V in electrochemical cell. Scan rate 20 mV s^{-1}, 0.1 M $HClO_4$, room temperature. Platinum loading is 35 and 20 μg_{Pt} cm^{-2} for 30 wt.% Pt_3Co/VC and 50 wt.% Pt/VC, respectively. Exposure to SO_2 was followed by 30 min purge in nitrogen. Arrows indicate onset potentials of sulfur oxidation at 0.8 V and peaks for sulfur oxidation at 1.2 V.

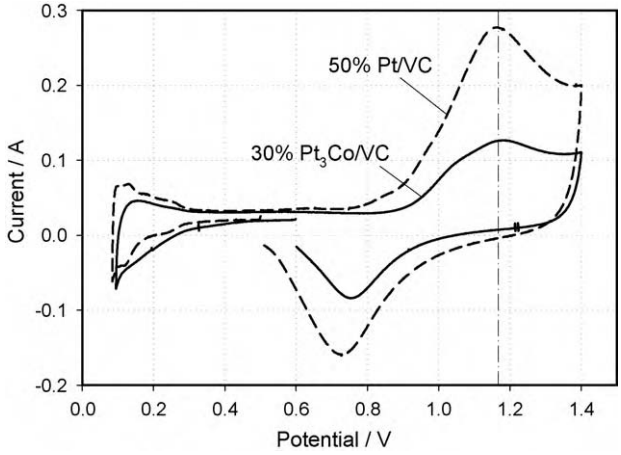

Fig. 13. The first CV curves measured after the contamination of 30 wt.% Pt_3Co/VC (solid) and 50 wt.% Pt/VC (dashed) cathodes with 1 ppm SO_2 in nitrogen at 0.6 and 0.5 V, respectively. Cell and humidifiers temperatures are 30 and 50 °C, respectively. The flow rate is 0.25|0.03 L min^{-1} (anode|cathode). Dashed line indicates peaks for sulfur oxidation at 1.17 V. Sulfur coverage is ~0.8 for both catalysts.

tion of oxygen species for 30 wt.% Pt_3Co/VC (0.75 V) is shifted in the positive direction with respect to 50 wt.%. Pt/VC (0.7 V). During the following eight scans, the peaks in the hydrogen and oxygen regions for the 50 wt.% Pt/VC develop to their original size observed in a clean solution. For the 30 wt.% Pt_3Co/VC, the peaks develop even further and become larger than the peaks observed in a clean solution, suggesting continuous cobalt leaching from the surface during oxidative sulfur removal. After seven scans, a ~7% increase in the area under hydrogen desorption region was observed for the 30 wt.% Pt_3Co/VC. The difference between scans 4 (blue) and 5 (red) is less pronounced for 30 wt.% Pt_3Co/VC than for 50 wt.% Pt/VC catalysts meaning that less CV sweeps are necessary to oxidize sulfur from the Pt_3Co/VC surface than from the Pt/VC surface. Sulfur coverages calculated by Eq. (4) are 0.84 ± 0.04 and 0.80 ± 0.04 for 30 wt.% Pt_3Co/VC and 50 wt.% Pt/VC catalysts, respectively.

Therefore, if SO_2 adsorption occurs on Pt_3Co/VC and Pt/VC catalysts with identical platinum ECSAs from solution in inert atmosphere, sulfur coverage and onset potentials for sulfur oxidation are also identical. An important question is whether this observation is transferable to SO_2 adsorption carried out in the fuel cell environment. Although it was not possible to make two cathodes with the same platinum ECSAs for Pt_3Co/VC and Pt/VC catalysts, it was feasible to prepare two cathodes with the same coverage of platinum surface by sulfur adatoms. Fig. 13 shows two CV scans recorded after SO_2 adsorption on 30 wt.% Pt_3Co/VC and 50 wt.% Pt/VC catalysts followed by 1 h purge in nitrogen. In order to get the same sulfur coverage of ~0.8 for both catalysts, the 50 wt.% Pt/VC and 30 wt.% Pt_3Co/VC cathode catalysts were exposed to 1 ppm SO_2 in nitrogen while holding cathode potentials at 0.5 and 0.6 V, respectively. In agreement with previous findings [7], sulfur coverage increases both with decreasing electrode potential and switching from oxygen-rich (air) to oxygen-free environment. For example, sulfur coverage of 0.83 ± 0.05 obtained during SO_2 adsorption from nitrogen at 0.6 V on 30 wt.% Pt_3Co/VC is higher than that of 0.57 ± 0.05 observed during SO_2 adsorption from air. Similarly, sulfur coverage of 0.80 ± 0.05 for SO_2 adsorption from nitrogen at 0.5 V on 50 wt.% Pt/VC is greater than 0.63 ± 0.05 [7] obtained in the same environment at 0.6 V.

In contrast to Fig. 12, the onset potentials measured for sulfur oxidation in Fig. 13 are not identical for 30 wt.% Pt_3Co/VC and 50 wt.% Pt/VC catalysts, with more negative onset potential for the latter catalyst. To be precise, there is a shoulder preceding the main wave of sulfur oxidation at 0.78–0.88 V that masks the onset potential for the main wave of sulfur oxidation. However, the peak position for sulfur oxidation to sulfate at 1.17 V is the same for both catalysts, which is consistent with what have been observed in Fig. 12.

Concluding this section, no shift in onset potentials and peak positions for sulfur oxidation for Pt_3Co/VC vs. Pt/VC catalysts were observed in SO_2 adsorption experiments in electrochemical cell, when catalysts with identical ECSAs were compared. In fuel cell experiments, performed at the same coverage of platinum surface by sulfur adatoms no shift in the peak position for sulfur oxidation was observed for Pt_3Co/VC vs. Pt/VC catalysts. It suggests that enhanced reactivity of Pt_3Co/VC catalyst with respect to S^0/SO_2 oxidation to sulfate is not due to lower adsorption energy of sulfur species on Pt_3Co nanoparticles.

4. Conclusions

1. Based on CO stripping and Cu-*upd* experiments, it is confirmed that a platinum-enriched layer or platinum "skeleton" [10,29] is formed on the surface of Pt_3Co nanoparticles under acidic environment. The difference between platinum ECSAs of Pt_3Co/VC and Pt/VC catalysts can be justified in terms of different particle sizes.
2. In agreement with previously reported RDE results [1], Pt_3Co/VC catalyst is more susceptive to SO_2 poisoning than Pt/VC at a given platinum loading. However, as evidenced by SO_2 adsorption from solution in an electrochemical cell, sulfur coverage is

Please cite this article in press as: O.A. Baturina, et al., Insights on the SO_2 poisoning of Pt_3Co/VC and Pt/VC fuel cell catalysts, Electrochim. Acta (2010), doi:10.1016/j.electacta.2010.06.004

identical on the two catalysts, if they have identical platinum ECSAs.

3. It is easier to oxidize S^0 or SO_2 adsorbed on the 30 wt.% Pt_3Co/VC catalyst than on the 50 wt.% Pt/VC catalyst, meaning than fewer CV cycles in inert atmosphere or polarization curves in air are needed to completely oxidize S^0/SO_2 from 30 wt.% Pt_3Co/VC than from 50 wt.% Pt/VC even though Pt_3Co/VC surface is more severely contaminated.
4. TPD experiments suggest a weaker platinum–sulfur bond for Pt_3Co/VC catalyst vs. Pt/VC in the gas phase, in agreement with DFT analysis [3].
5. Even though results of TPD experiments suggest weaker platinum–sulfur bond for Pt_3Co/VC catalyst vs. Pt/VC in the gas phase, we do not find an evidence for a weaker sulfur adsorption on the former catalyst in electrochemical experiments performed both in electrochemical cell and FCs. The same onset potentials and peak positions for sulfur oxidation are observed for both catalysts having the same coverage of sulfur adatoms at electrode/solution interface (see Fig. 12). The same peak positions for sulfur oxidation are observed for both catalysts having the same coverage of sulfur adatoms in a FC environment (see Fig. 13). We assume that enhanced reactivity of Pt_3Co/VC catalyst with respect to S^0/SO_2 oxidation to sulfate is not due to a weaker Pt–S bond, but has to do either with a higher mobility of adsorbed oxygen species or higher reactivity of vacancies present on cobalt-leached alloy surface towards dissociation of H_2O or molecular oxygen. Adsorbed $O[H]_{ads}$ species are mandatory for sulfur oxidation to sulfate at potentials higher than 1 V in inert atmosphere [39,40]. Since the sulfur oxidation reaction occurs on the surface partially covered with adsorbed oxygen, its higher mobility would provide higher sulfur oxidation rate. A greater number of vacancies on Pt_3Co/VC catalyst with "skeleton" or platinum-enriched surface would facilitate water dissociation to OH_{ads} and adsorbed oxygen, as well as molecular oxygen dissociation when SO_2 oxidation in air is considered. Although we cannot exclude a particle size effect, as the particle size is larger on the 30 wt.% Pt_3Co/VC (4.3 ± 0.5 nm) than on the 50 wt.% Pt/VC (2.9 ± 0.5 nm) catalyst, enhanced S^0/SO_2 oxidation to sulfate on 30 wt.% Pt_3Co/VC vs. 20 wt.% Pt/VC was also observed, when particles of closer sizes were considered [1].
6. TPD spectra may be used to detect cobalt on the surface of Pt_3Co nanoparticles.

Acknowledgments

The authors are grateful to the Office of Naval Research for financial support of this project. BG is an American Society of Engineering Education Postdoctoral Fellow.

References

[1] Y. Garsany, O.A. Baturina, K.E. Swider-Lyons, J. Electrochem. Soc. 156 (2009) B848.
[2] Y. Garsany, O.A. Baturina, K.E. Swider-Lyons, J. Electrochem. Soc. 154 (2007) B670.
[3] D. Pillay, M.D. Johannes, Y. Garsany, K.E. Swider-Lyons, J. Phys. Chem. C 114 (2010) 7822.
[4] D. Pillay, M.D. Johannes, J. Phys. Chem. C 112 (2008) 1544.
[5] V. Stamenkovic, B.S. Mun, K.J.J. Mayrhofer, P.N. Ross, N.M. Markovic, J. Rossmeisl, J. Greeley, J.K. Norskov, Angew. Chem. Int. Ed. 45 (2006) 2897.
[6] T.D. Gladysheva, B.I. Podlovchenko, Vestn. Moskov. Univ. Ser. 2 Khimiya (Rus.) 38 (1997) 3.
[7] O.A. Baturina, K.E. Swider-Lyons, J. Electrochem. Soc. 156 (2009) B1423.
[8] H.A. Gasteiger, S.S. Kocha, B. Sompalli, F.T. Wagner, Appl. Catal. B: Environ. 56 (2005) 9.
[9] B.B. Damaskin, O.A. Petrii, Introduction into Electrochemical Kinetics, Vysshaya Shkola, USSR, Moscow, 1983.
[10] V.R. Stamenkovic, B.S. Mun, K.J.J. Mayrhofer, P.N. Ross, N.M. Markovic, J. Am. Chem. Soc. 128 (2006) 8813.
[11] M. Arenz, K.J.J. Mayrhofer, V. Stamenkovic, B.B. Blizanac, T. Tomoyuki, P.N. Ross, N.M. Markovic, J. Am. Chem. Soc. 127 (2005) 6819.
[12] T. Sato, K. Kunimatsu, H. Uchida, M. Watanabe, Electrochim. Acta 53 (2007) 1265.
[13] K.J.J. Mayrhofer, D. Strmcnik, B.B. Blizanac, V. Stamenkovic, M. Arenz, N.M. Markovic, Electrochim. Acta 53 (2008) 3181.
[14] N.M. Markovic, B.N. Grgur, C.A. Lucas, P.N. Ross, J. Phys. Chem. B 103 (1999) 487.
[15] C.L. Green, A. Kucernak, J. Phys. Chem. B 106 (2002) 1036.
[16] T.D. Gladyshev, B.I. Podlovchenko, Z.A. Zikrina, Sov. Electrochem. (Rus.) 23 (1987) 1356.
[17] B.D. Gould, O.A. Baturina, K.E. Swider-Lyons, J. Power Sources 188 (2009) 89.
[18] S. Kocha, in: W. Veilstich, A. Lamm, H.A. Gasteiger (Eds.), Handbook of Fuel Cells: Fundamentals, Technology, Applications, vol. 3, Wiley & Sons, Weinhem, 2003 (Ch. 43).
[19] H.A. Gasteiger, W. Gu, R. Makhatia, M.F. Mathias, B. Sompalli, in: W. Veilstich, A. Lamm, H.A. Gasteiger (Eds.), Handbook of Fuel Cells – Fundamentals, Technology and Applications, vol. 3, Wiley & Sons, Weinhem, 2003 (Ch. 46).
[20] O.A. Baturina, Y. Garsany, T.J. Zega, R.M. Stroud, T. Schull, K.E. Swider-Lyons, J. Electrochem. Soc. 155 (2008) B1314.
[21] U.A. Paulus, A. Wokaun, G.G. Scherer, T.J. Schmidt, V. Stamenkovic, V. Radmilovic, N.M. Markovic, P.N. Ross, J. Phys. Chem. B 106 (2002) 4181.
[22] T. Toda, H. Igarashi, H. Uchida, M. Watanabe, J. Electrochem. Soc. 146 (1999) 3750.
[23] S. Koh, J. Leisch, M.F. Toney, P. Strasser, J. Phys. Chem. C 111 (2007) 3744.
[24] S. Koh, C. Yu, P. Mani, R. Srivastava, P. Strasser, J. Power Sources 172 (2007) 50.
[25] S. Chen, W.C. Sheng, N. Yabuuchi, P.J. Ferreira, L.F. Allard, Y. Shao-Horn, J. Phys. Chem. C 113 (2009) 1109.
[26] K.J.J. Mayrhofer, B.B. Blizanac, M. Arenz, V.R. Stamenkovic, P.N. Ross, N.M. Markovic, J. Phys. Chem. B 109 (2005) 14433.
[27] K.J.J. Mayrhofer, V. Juhart, K. Hartl, M. Hanzlik, M. Arenz, Angew. Chem. Int. Ed. 48 (2009) 3529.
[28] G. Garcia, J.A. Silva-Chong, O. Guillen-Villafuerte, J.L. Rodriguez, E.R. Gonzalez, E. Pastor, Catal. Today 116 (2006) 415.
[29] M. Wakisaka, S. Mitsui, Y. Hirose, K. Kawashima, H. Uchida, M. Watanabe, J. Phys. Chem. B 110 (2006) 23489.
[30] F. Maillard, M. Eikerling, O.V. Cherstiouk, S. Schreier, E. Savinova, U. Stimming, Faraday Discuss. 125 (2004) 357.
[31] A.I. Danilov, E.B. Molodkina, Y.M. Polukarov, Russ. J. Electrochem. 34 (1998) 1249.
[32] O. Savadogo, A. Essalik, J. Electrochem. Soc. 143 (1996) 1814.
[33] Y. Garsany, O.A. Baturina, S.S. Kocha, K. E. Swider-Lyons, Analyt. Chem. (in press), doi:ac 100306c.
[34] T. Loucka, J. Electroanal. Chem. 31 (1971) 319.
[35] S. Thomas, Y.E. Sung, H.S. Kim, A. Wieckowski, J. Phys. Chem. 100 (1996) 11726.
[36] Y. Nagahara, S. Sugawara, K. Shinohara, J. Power Sources 182 (2008) 422.
[37] V. Stamenkovic, T.J. Schmidt, P.N. Ross, N.M. Markovic, J. Phys. Chem. B 106 (2002) 11970.
[38] D. Fenske, W.L. Yim, S. Neuendorf, D. Hoogestraat, D. Greshnykh, H. Borchert, T. Kluner, K. Al-Shamery, Chemphyschem 8 (2007) 654.
[39] C. Korzeniewski, W. McKenna, S. Pons, J. Electroanal. Chem. 235 (1987) 361.
[40] K.I. Rozental, V.I. Veselovskii, Zh. Fiz. Khim. (Rus.) 27 (1953) 1163.

Please cite this article in press as: O.A. Baturina, et al., Insights on the SO_2 poisoning of Pt_3Co/VC and Pt/VC fuel cell catalysts, Electrochim. Acta (2010), doi:10.1016/j.electacta.2010.06.004